

A New Fragment Contribution-Corresponding States Method for Physicochemical Properties Prediction of Ionic Liquids

Ying Huang

Beijing Key Laboratory of Ionic Liquids Clean Process, State Key Laboratory of Multiphase Complex Systems, Key Laboratory of Green Process and Engineering, Institute of Process Engineering, Chinese Academy of Sciences, Beijing 100190, P.R. China

College of Chemistry and Chemical Engineering, University of Chinese Academy of Sciences, Beijing 100049, P.R. China

Haifeng Dong, Xiangping Zhang, Chunshan Li, and Suojia Zhang

Beijing Key Laboratory of Ionic Liquids Clean Process, State Key Laboratory of Multiphase Complex Systems, Key Laboratory of Green Process and Engineering, Institute of Process Engineering, Chinese Academy of Sciences, Beijing 100190, P.R. China

DOI 10.1002/aic.13910

Published online October 18, 2012 in Wiley Online Library (wileyonlinelibrary.com).

A new fragment contribution-corresponding states (FC—CS) method based on the group contribution method and the corresponding states principle is developed to predict critical properties of ionic liquids (ILs). There are 46 fragments specially classified for ILs considering the ionic features of ILs, and the corresponding fragment increments are determined using the experimental density data. The accuracy of the developed method is verified indirectly via predicting density and surface tension of ILs. The results show that the FC—CS method is reasonable with an average absolute relative deviation less than 4%. With the calculated critical properties, corresponding states heat capacity (CSHC) and corresponding states thermal conductivity (CSTC) correlations are proposed to predict heat capacity and thermal conductivity of ILs, respectively. The predicted results agreed well with the experimental data. The proposed FC—CS method and the two corresponding states correlations are important for design, simulation, and analysis of new ionic liquid processes. © 2012 American Institute of Chemical Engineers AIChE J, 59: 1348–1359, 2013

Keywords: ionic liquids, fragment contribution-corresponding states method, density, heat capacity, thermal conductivity

Introduction

Ionic liquids (ILs), which refer to liquids that are entirely composed of ions, attract increasing interest in both academic research and the industry.¹ The widespread applications of ILs have been reported in numerous and diverse fields such as chemical and biological catalysis reactions,^{2,3} electrochemical industry,⁴ analytical chemistry,⁵ energy and fuel cycle,⁶ and separation engineering.⁷ With increasing potentials of ionic liquids for industrial applications being explored, knowledge of the physicochemical properties of ILs has become crucial. It was estimated that at least 10¹⁸ ILs (binary and ternary mixtures are included) can be potentially created¹ with the different combinations of anions and cations and modification of side chains, thus, measuring all the properties of various ILs under a wide range of conditions through experimental techniques is impractical. Alternatively, generalized reliable predictive methods for the

physicochemical properties are fundamentally important for the development and design of new IL-based processes.

A brief survey on the current methods for predicting properties of ILs shows that there are four main methods developed (1) models based on quantum chemistry, (2) empirical correlations based on the adjustable parameters for specific IL, (3) the group contribution method (GCM), and (4) correlations based on the concept of corresponding states principle (CSP). Some applications of these four methods are provided in Table 1. The quantitative structure–property relationship (QSPR) method based on *ab initio* calculations was first presented for the prediction of the melting point and liquid density of one kind of energetic IL.⁸ Then, Sun et al.⁹ calculated another two kinds of ILs using a QSPR approach. The COSMO—RS method, which was originally used in phase equilibrium calculations, was extended for the prediction of the physicochemical properties of ILs, such as density,¹⁰ viscosity, surface tension,¹¹ vapor pressure and vaporization enthalpy.¹² Although the methods above were derived at the atomic and molecular levels, they are very expensive in computation for large compounds and their accuracy range irregularly. Many studies have used empirical correlations to predict density,^{13,14} viscosity, interfacial tension, self-diffusion coefficient, refractive index,¹⁵ and thermal

Additional Supporting Information may be found in the online version of this article.

Correspondence concerning this article should be addressed to C. Li at csli@home.ipe.ac.cn and S. Zhang at sjzhang@home.ipe.ac.cn.

Table 1. Summary of Property Prediction of ILs by Four Types of Methods

Methods Type	Specific Method	Property	T(K)	P(MPa)	Number of ILs	Predictive Deviations	Reference
1 Quantum chemistry-based	QSPR	Melting point Density	–	–	26	^a R > 0.9	Trohalaki et al. ⁸
	COSMO-RS	Melting point Density Viscosity Surface tension Vapor pressure Density	– 298 298 313 437–517 292–391	– 0.1 0.1 0.1 0.1 0.1	41 40 10 4 6	^a R > 0.9 ^a R > 0.99 – ^b RD = 10% –	Sun et al. ⁹ Palomar et al. ¹⁰ Torrecilla et al. ¹¹ Diedenhofen et al. ¹² Jacquemin et al. ¹³
2 Empirical correlations	$\rho = a + b(T - 273.15)$ $\rho = \frac{\rho_0}{1 - C_T \ln((B_T + p)/(B_T + p_0))}$ $\eta_{calc} = \eta_0 \exp[B/(T - C)]$ $D_{+/-} = D_{0,+/-} \exp\left(-\frac{E_{A,+/-}}{RT}\right)$ $\eta_{calc} = n_0 + n_1 T + \frac{\Delta \eta}{\Delta T} (\lambda - \lambda_D)$ $\lambda_{c,calc} = \lambda_0 + \lambda_1 T$	Density Viscosity Self-diffusion coefficients Refractive index Thermal conductivity Density	283–333 283–363 313–363 283–313 273–353 253–473	0.1–65 0.1 0.1 0.1 0.1 0.1–300	5 1 1 1 10 828	^c RRD < 0.009 ^c RRD = 1.37 % – ^c RRD = 0.004% ^d AARD = 7% ^d AARD = 0.53%	Guerrero et al. ¹⁴ Koller et al. ¹⁵ Koller et al. ¹⁵ Koller et al. ¹⁵ Froeba et al. ¹⁶ Paduszynski et al. ¹⁸
3 The group contribution method	$\rho(T, P) = \frac{\rho(T, P_0)}{1 - C \ln[1 + (P - P_0)B(T)]}$ $\ln \eta = A_\eta + \frac{B_\eta}{(T - T_{0\eta})}$ $\kappa = A_\kappa - B_\kappa T$	Viscosity Thermal conductivity Density	293–393 293–390 270–360	0.1 0.1 0.1	29 16 146	^d AARD = 8% ^d AARD = 1.06% ^d AARD = 2.6%	Gardas et al. ¹⁹ Gardas et al. ¹⁹ Valderrama et al. ²⁸
4 Corresponding states principle-based equations	$\rho = A/B + (2/7)[A(\ln B)/B][[(T - T_b)/(T_c - T_b)]]$ $\gamma = 0.819 \left(\frac{T_b - T}{T_b - T_m} \right) \gamma_m + 0.500 \left(\frac{T}{T_b} \right) \gamma_m$ $\frac{C_p - C_p^0}{R} = 1.586 + \frac{0.49}{1 - T_r} + \frac{6.3(1 - T_r)^{1/3}}{T_r} + \frac{0.4355}{1 - T_r}$	Surface tension Heat capacities	278–473 256–470	0.1 0.1	30 53	^d AARD = 2.98% ^d AARD = 2.9%	Mousazadeh et al. ²⁹ Ge et al. ³⁰

^aR: correlation coefficients.

^bRD: relative deviation.

^cRRD: relative root-mean-square deviations.

^dAARD: average absolute relative deviation.

^eSpecific method: meaning and units of notations in each equation can be found in cited references.

Table 2. Predictive Methods for Critical Parameters of ILs

Method	Critical parameters	Number of ILs	Predictive deviations	Authors	Year
Eotvos and Guggenheim surface tension equations	T_c	15	—	Rebelo et al. ³²	2005
		17	—	Kilaru et al. ³⁴	2007
		34	—	Ghatee et al. ³⁵	2010
		4	—	Weiss et al. ³³	2010
A modified group contribution method	T_c, P_c, V_c, ω	50	AARD = 5.2%	Valderrama et al. ³⁷	2007
		294	AARD = 3.9%	Valderrama et al. ³⁸	2009
		747	AARD = 4.4%	Shen et al. ¹⁷	2011

conductivity¹⁶ of ILs. Their predictive results were highly in accordance with the experimental results, whereas sufficient experimental data under various conditions are required to fit different parameters of expression of each IL. GCM is a kind of semiempirical theory which is extensively used for estimating properties such as critical properties,¹⁷ density,¹⁸ viscosity, electrical conductivity and thermal conductivity¹⁹ of ILs. This method is easy to use, but many of the reported GCMs are based on the groups of molecular compounds. The corresponding states principle proposed by van der Waals in 1873 was particularly helpful for the property estimation of widespread substances.²⁰ The extended correlations of van der Waals's CSP, including the equation of state, have been applied to successfully predict various properties of molecular compounds and inorganic salts, such as density,²¹ vapor pressure, entropy of evaporation, heat capacity, surface tension,^{22,23} thermal conductivity,²⁴ and viscosity.^{25–27} However, reports on the application of the CSP to ILs are few. Valderrama et al.²⁸ proposed an empirical CSP density correlation for ILs which showed greater accuracy compared with 10 generalized CSP correlations for molecular fluids available in other studies. Mousazadeh et al.²⁹ related the reduced surface tensions to the reduced temperatures using a linear regression relationship based on the CSP. Ge and Hardacre³⁰ predicted ideal gas heat capacity using the Joback GCM and calculated the liquid heat capacity of ILs using an original CSP correlation. However, the ideal gas heat capacity of ILs cannot be tested using experimental data; thus, the Joback GCM may place a level of uncertainty on the prediction of the liquid heat capacity of ILs. CSP is hampered in its application to ILs mainly because of the absence of critical parameters that are unavailable through direct experimental observations, since ILs generally degrade below their critical temperatures. Critical properties are used not only as the basis for models such as corresponding states correlations for PVT equations of state, but also in composition-dependent mixing rules for the parameters on describing mixtures.²⁰ Thus, it is imperative to predict the critical properties of ILs through reliable method.

Two methods have been reported for predicting critical properties of ILs, as summarized in Table 2. One is Eotvos and Guggenheim method; the other is the group contribution method. Eotvos³¹ and Guggenheim²² empirical surface tension equations, which describe the behavior of the liquid-vapor interfacial tension γ as a function of temperature (T), provide critical temperature (T_c) via the extrapolation of sufficient $\gamma(T)$ data to the temperature at which $\gamma = 0$. Rebelo et al.³² tested the adequacy of the two aforementioned equations by predicting the T_c of 90 compounds. Their results showed that both expressions could provide an accurate T_c estimate for most fluids, except the strongly hydrogen-bonded substances and several inorganic molten salts. More-

over, they first extended the two equations to estimate the critical temperature of ILs. Several researchers^{33–35} subsequently quoted the Eotvos and Guggenheim equations and calculated the T_c of ILs. These pioneering works provide ideas and methods for predicting the critical temperatures of ILs, whereas the derived values needed further investigations to justify their validity. Weiss et al.³⁶ pointed out the existence of uncertainties on the direct application of either Eotvos or Guggenheim expression to determine the T_c of ILs. They stated the surface tension of an IL as a function of temperature might exhibit an inflection point, and the extrapolation of surface tension to its vanishing temperature was error-prone. Moreover, the two equations are unavailable for determining the acentric factor (ω), the critical pressure (P_c), and the critical volume (V_c), which are all necessary for the CSP.

The GCM is the main method used for estimating critical properties,²⁰ and only two articles have devoted themselves to predicting the entire critical parameters of ILs by far. Valderrama and Robles³⁷ first used a modified GCM based on the well-known Lydersen and Joback and Reid's method to predict the critical properties, normal boiling temperatures, and acentric factors of 50 ILs. The accuracy of their method was justified by calculating the liquid densities through a generalized correlation. Shen et al.¹⁷ developed a GC–PT method which combined the modified Lydersen-Joback-Reid GCM³⁸ with the Patel-Teja (PT) equation of state to predict the critical parameters of ILs, and they confirmed the results by predicting the densities at higher temperature and pressure conditions using four different density correlations. Undeniably, the studies above^{17,38} have given values of critical parameters, at least reliable for the prediction of IL densities. Nevertheless, their suitability for the prediction of other properties remains unknown and the used groups did not contain ionic groups which are the main components in ILs. As Jones et al.³⁹ pointed out, the T_c values from the work of Valderrama and Robles³⁷ were likely to be in error because of the noninclusion of the Coulombic energy in IL. Therefore, a more exact predictive method for critical parameters of ILs considering their ionic features should be developed urgently. Thus, generalized equations based on CSP for the calculation of physicochemical properties will be accessible for the fundamental data and industry field.

This study mainly focuses on two respects. In one respect, a FC–CS method is developed to estimate the critical properties, normal boiling temperatures, and acentric factors of ILs. The validity and accuracy of the FC–CS method is verified via the prediction of density and surface tension using CSP equations. In another respect, new heat capacity and thermal conductivity predictive correlations based on the CSP were proposed for ILs as an extended application of the FC–CS method.

Table 3. Summary of Experimental Data

Property	Temperature Range (K)	Pressure Range (MPa)	Number of ILs	Data Points
Density	283.15–313.2	0.1	490	514
Density	273.15–473.15	0.1	519	1907
Density	278.15–428.15	0.1–100	128	3272
Surface tension	273.15–492.5	0.1	112	838
Heat capacity	10–573.1	0.1	26	599
Thermal conductivity	273.15–390	0.1–20	22	138

Database

In this study, all experimental data were extracted from IL Thermo Database,⁴⁰ a book,⁴¹ Database software,⁴² three main references,^{17,30,43} and other accessible studies on the physicochemical properties of ILs. The principle of screening experimental data from a sufficient amount of literature is to discard the data that deviate from other data. For example, the surface tension of 1-Butyl-3-methylimidazolium tetrafluoroborate has been reported in at least 17 various studies.⁴³ Two experimental data of those studies^{44,45} were rejected in the current study because of enormous data discrepancy compared with the others at 298.15 K. All literature sources have been listed in the Supplementary Material to provide direct and comprehensive information. Table 3 summarized the total number of ILs, data points, and the condition of different experimental property data used in this work.

The investigated ILs were mainly based on alkyl-substituted cations, including imidazolium [Im], pyridinium [Py], pyrrolidinium [Pyr], piperidinium [Pip], guanidinium [Gua], phosphonium [P], ammonium [N], sulfonium [S], and different anions, such as tetrafluoroborate [BF₄], hexafluorophosphate [PF₆], halide [X], bis(trifluoromethylsulfonyl)imide [BTI], bis(perfluoroethyl sulfonyl)imide [BETI], alkyl sulfate [RSO₄], dialkylphosphate [R₂PO₄], trifluoromethylsulfonate [TfO], trifluoroacetate [TfA], nitrate [NO₃], dicyanamide [Dca], tricyanomethanide [Tcm], tris(trifluoromethylsulfonyl)methide [Tf₃C], tetrachloroaluminate [AlCl₄], tetrachloroironate [FeCl₄], tetrachlorogallate [GaCl₄], tetrachloroindate [InCl₄], trichlorozincate [ZnCl₃], and acetate [Ac], among others.

The classification of IL fragments, the molar mass, the global formula, the IUPAC name and the abbreviations of ILs are presented in the Supplementary Material. In addition, all predictive critical properties, density, surface tension, heat capacity, and thermal conductivity are also included in the Supplementary Material. Given this information, any reader can search for the required property data and easily calculate the physicochemical properties of any IL composed of the fragments defined in this study.

Methodology

A FC—CS method

The definition of fragments of ILs. In this study, with the simultaneous consideration of the ionic features and neutral portion of ILs, each IL is divided into three basic elements, namely, cation fragment, anion fragment, and substituent fragment attached to the cation or anion. The definition of fragments is proposed to distinguish with original GCM which is applied to organic compounds. A complete set of 46 fragments, including 7 cation fragments, 18 anion fragments, and 21 substituent fragments were defined. Figure 1 shows the chemical structures of the cation fragments belonging to the ILs investigated in this study. The structures of anion and substituent fragments are presented in the Supplementary Material.

Description of the Method. A new FC—CS method proposed based on a CSP correlation and the GCM consists of six equations (1) the Riedel corresponding states equation⁴⁶ (see Eq. 1) for calculating density (ρ), (2) the Joback-Reid GCM⁴⁷ (see Eq. 2) for calculating T_b , (3) the GCM modified by Alvarez and Valderrama⁴⁸ (see Eq. 3) for calculating T_c , (4) the Lydersen GCM²⁰ (see Eq. 4) for calculating P_c , (5) the MXXC method⁴⁹ (see Eq. 5) for calculating V_c , and (6) the equation (see Eq. 6) deduced in this study from the Clausius-Clapeyron equation and the acentric factor equation of definition²⁰ for calculating ω . The density calculated by Eq. 1 is based on T_c , V_c and ω , and ω is calculated based on T_b , T_c and P_c . Therefore, the six property parameters can be associated with the FC—CS method which can be described as follows

$$\rho = \frac{M}{V_c} [1 + 0.85(1 - T_r) + (1.6916 + 0.984\omega)(1 - T_r)^{1/3}] \quad (1)$$

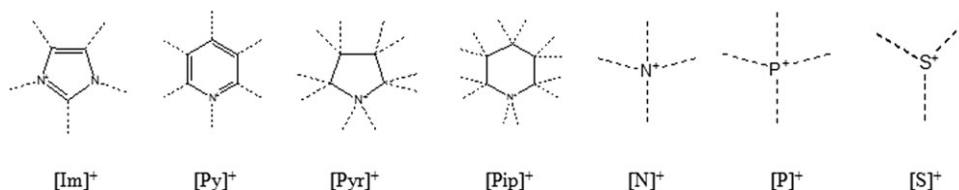
$$T_b = 198.2 + \sum_i n_i \Delta T_{b,i} \quad (2)$$

$$T_c = \frac{T_b}{0.5703 + 1.0121 \sum_i n_i \Delta T_{c,i} - \left(\sum_i n_i \Delta T_{c,i} \right)^2} \quad (3)$$

$$P_c = \frac{M}{\left(0.34 + \sum_i n_i \Delta P_{c,i} \right)^2} \quad (4)$$

$$V_c = 28.8946 + 14.75246 \sum_i n_i \Delta V_{c,i} + \frac{6.03853}{\sum_i n_i \Delta V_{c,i}} \quad (5)$$

$$\omega = \frac{T_b T_c}{(T_c - T_b)(0.7 T_c)} \log \left(\frac{P_c}{P_b} \right) - \left(\frac{T_c}{T_c - T_b} \right) \log \left(\frac{P_c}{P_b} \right) + \log \left(\frac{P_c}{P_b} \right) - 1 \quad (6)$$


Figure 1. Cation fragments of ILs.

In Eqs. 1–4, n_i represents the number of fragment i that appears in the ILs; $\Delta T_{b,i}$, $\Delta T_{c,i}$, $\Delta P_{c,i}$, and $\Delta V_{c,i}$ denote the fragment increments of fragment i for the normal boiling temperature, critical temperature, critical pressure, and critical volume, respectively. In Eq. 5, P_b is the atmospheric pressure in bar. In Eq. 6, M is the molar mass in $\text{g}\cdot\text{mol}^{-1}$, and T_r is the reduced temperature ($T_r = T/T_c$).

Determination of fragment increments

As previously described, 46 fragments were defined for the ILs investigated in this study. Their corresponding fragment increments (namely, $\Delta T_{b,i}$, $\Delta T_{c,i}$, $\Delta P_{c,i}$, and $\Delta V_{c,i}$) for calculating T_b , T_c , P_c , and V_c were performed by optimizing the following objective function

$$O.F. = \min \sum_{i=1}^{N_p} (\rho_i^{\text{cal}} - \rho_i^{\text{exp}})^2 \quad (7)$$

The density data used to determine the fragment increments were under the conditions with temperatures of approximately 298 K or 293 K and pressure of 101.325 kPa.

The average absolute relative deviation (AARD) can be defined as follow

$$\text{AARD} (\%) = 100 \times \sum_{i=1}^{N_p} |\rho_i^{\text{cal}}/\rho_i^{\text{exp}} - 1.0|/N_p \quad (8)$$

where N_p represents the total number of data points of density, ρ is the density in $\text{g}\cdot\text{cm}^{-3}$, and superscripts “cal” and “exp” denote the calculated values using the FC–CS method and the experimental data, respectively.

Verification of the FC–CS method

Verification of the FC–CS method via density prediction. In order to test the validity of the fragment increments as well as the FC–CS method developed in this study, the liquid densities over a wide range of temperature and pressure were estimated using six different equations, including the Riedel equation (see Eq. 1), VSD equation⁵⁰ (see Eq. 9), VSY equation⁵⁰ (see Eq. 10), LGM²⁸ (see Eq. 11), Yamada-Gunn equation⁵¹ (YG) (see Eq. 12), and McHaweh equation⁵² (MH) (see Eq. 13). These density equations are all based on the CSP. The calculation method for the AARD of the different methods is similar to Eq. 8

$$\rho = \frac{Mp_c}{RT_c} \left(\frac{0.3445p_c V_c^{1.0135}}{RT_c} \right)^{\Omega}; \quad \Omega = - \left[\frac{1 + (1 - T_r)^{2/7}}{1 + (1 - T_{br})^{2/7}} \right] \quad (9)$$

$$\rho = \left(0.01256 + \frac{0.9533M}{V_c} \right) \left[\left(\frac{0.0039}{M} + \frac{0.2987}{V_c} \right) V_c^{1.033} \right]^{\Psi}; \quad \Psi = - \left(\frac{1 - T_r}{1 - T_{br}} \right)^{2/7} \quad (10)$$

$$\rho = A/B + (2/7)[A(\ln B)/B][(T - T_b)/(T_c - T_b)] \quad (11)$$

$$A = 0.3411 + 2.0443M/V_c \quad (11a)$$

$$B = (0.5386/V_c + 0.0393/M)V_c^{1.0476} \quad (11b)$$

$$\rho = \frac{M}{V_c} (0.29056 - 0.08775\omega)^{-(1-T_r)^{2/7}} \quad (12)$$

$$\rho(T) = \frac{M}{V_c} (1 + 1.169\tau^{1/3} + 1.818\tau^{2/3} - 2.658\tau + 2.161\tau^{4/3}) \quad (13)$$

$$\tau = 1 - \frac{(T/T_c)}{[1 + m(1 - \sqrt{T/T_c})]^2} \quad (13a)$$

$$m = 0.480 + 1.574\omega - 0.176\omega^2 \quad (13b)$$

where T_{br} is the reduced temperature at the normal boiling point ($T_{br} = T_b/T_c$).

Verification of the FC–CS Method via Surface Tension. CSP correlations are successful in the surface tension estimation of a substantial amount of molecular liquids.^{53–56} Surface tension values of ILs are similar to most molecular liquids. In this study, two frequently-used corresponding states surface tension correlations were adopted to predict the surface tension of ILs by virtue of the critical parameters obtained using the FC–CS method. The two equations proposed by Brock-Bird⁵⁶ and Pitzer²⁰ are described as follows

$$\sigma = P_c^{2/3} T_c^{1/3} (1 - T_r)^{11/9} Q; \quad Q = 0.1196[1 + T_{br} \ln(P_c/1.01325)/(1 - T_{br})] - 0.279 \quad (14)$$

$$\sigma = P_c^{2/3} T_c^{1/3} \frac{1.86 + 1.18\omega}{19.05} \left[\frac{3.75 + 0.91\omega}{0.291 - 0.08\omega} \right]^{2/3} (1 - T_r)^{11/9} \quad (15)$$

The AARD is defined as follows

$$\text{AARD} (\%) = 100 \times \sum_{i=1}^{N_p} |\sigma_i^{\text{cal}}/\sigma_i^{\text{exp}} - 1.0|/N_p \quad (16)$$

CSHC correlation

The CSP correlation of liquid heat capacity (C_p) requires an ideal gas heat capacity value²⁰ which are not accessible for ILs through experiment. To the best of our knowledge, corresponding states correlation for the liquid heat capacity estimation of IL has not been reported to date. Based on the critical parameters, a new corresponding states heat capacity (CSHC) correlation is proposed as follows

$$C_p = M\omega T^a T_c^b \left[c + \left(\frac{1 - T_{br}}{1 + T_r} \right)^d \right] / P_c^e \quad (17)$$

$$a = 1.565, \quad b = 0.15, \quad c = -0.00005, \quad d = 4.126, \quad e = 0.7568$$

The constants a , b , c , d , and e were estimated by minimizing the following objective function

$$O.F. = \sum_{i=1}^{N_p} (C_{p_i}^{\text{cal}} - C_{p_i}^{\text{exp}})^2 \quad (18)$$

The AARD can be defined as follows

$$\text{AARD} (\%) = 100 \times \sum_{i=1}^{N_p} |C_{p_i}^{\text{cal}}/C_{p_i}^{\text{exp}} - 1.0|/N_p \quad (19)$$

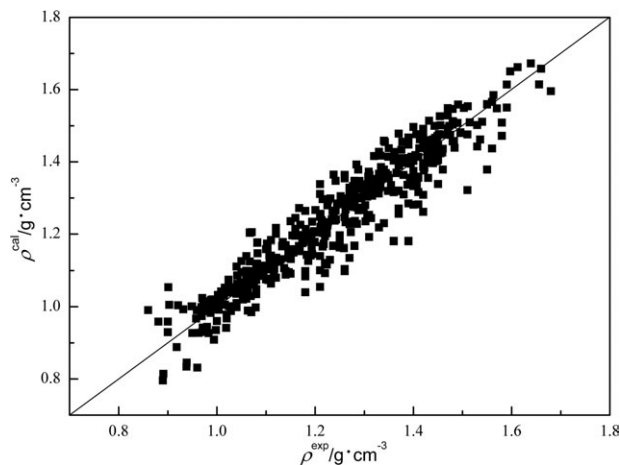
Table 4. Fragment Increments for the FC–CS Method

No.	Fragments	$\Delta T_{b,i}$	$\Delta T_{c,i}$	$\Delta p_{c,i}$	$\Delta V_{c,i}$
Cation fragments					
1	im	89.58	0.07	0.81	3.92
2	pyr	−86.00	0.0911	−0.122	−14.6
3	py	102.46	0.0701	0.7749	2.4475
4	pip	8.49	0.01	−0.52	−13.79
5	N	156.80	0.0899	0.589	4.615
6	P	349.70	0.078	−0.011	9.925
7	S	21.89	0.06	1.43	8.30
Anion fragments					
8	[BF ₄] [−]	102.53	0.14	−0.12	4.37
9	[PF ₆] [−]	195.29	0.1466	0.3072	10.023
10	[Cl] [−]	96.56	0.127	−0.6717	−1.5871
11	[Br] [−]	79.49	0.1635	−0.04001	1.081
12	[I] [−]	155.33	0.161	0.07014	5.725
13	[NO ₃] [−]	84.58	0.1455	−0.3091	0.9915
14	[Ace] [−]	13.58	0.2545	0.69952	14.13
15	[BMB] [−]	51.71	0.1282	1.397	22.55
16	[BMLB] [−]	30.71	0.1322	1.747	27.68
17	[BOB] [−]	30.51	0.1254	0.977	13.58
18	−CN	57.71	0.1351	−0.59	−3.11
19	−SO ₂ −	40.85	0.1639	−0.4901	−2.7086
20	−P=O	−16.52	0.194	−0.64	−3.983
21	In	19.41	0.3054	4.006	26.91
22	Zn	−7.56	0.438	2.245	17.91
23	Ga	−3.78	0.3202	3.711	24.88
24	Fe	1.22	0.3115	3.718	23.91
25	Al	−11.56	0.3366	3.355	24.257
Substituent fragments					
26	−CH ₃	41.24	−0.02	0.32	5.93
27	−CH ₂ −	6.17	0.00	0.20	3.42
28	>CH− or [−CH−] [−]	21.58	0.03	0.05	1.90
29	>C< or [>C−] [−]	17.41	0.38	1.96	22.13
30	=CH ₂	7.58	−0.18	1.51	−1.47
31	=CH−	7.25	0.14	−1.48	−1.33
32	=C<	47.58	−1.08	−2.21	−19.31
33	−H (ring)	47.00	0.00	0.21	4.01
34	−O− or [−O] [−]	22.49	−0.005	0.133	2.6685
35	=O	−205.16	0.058	−0.102	−0.2195
36	−OH	188.50	−0.0062	0.2181	5.614
37	−H(non−ring)	41.89	0.07	0.62	8.53
38	−S or [−S] [−]	35.41	0.01	0.30	6.89
39	BF ₃	79.15	0.17	−0.22	−0.20
40	benzene ring	−13.58	−0.0694	0.0702	−4.015
41	[−N−] [−] or >N−	37.79	0.5992	0.8077	11.114
42	−NH ₂	70.86	−0.0232	0.2319	2.303
43	C=O	50.86	0.165	−0.7206	−2.883
44	>CF−	−121.56	−0.0323	−0.5344	−2.044
45	−CF ₂ −	17.57	−0.0053	0.3954	5.223
46	−CF ₃	45.04	−0.0348	0.78925	10.00081

CSTC correlation

Latini method and Sastri method are the two main methods for predicting thermal conductivity (λ) of organic compounds.²⁰ Latini method was recommended for substances having molar masses between 50 g·mol^{−1} and 250 g·mol^{−1} with an error of less than 10%.²⁰ However, the molar masses of many ILs are larger than 250 g·mol^{−1}. The Sastri method²⁰ is a kind of GCM with group parameters that are unavailable for ILs. In this study, a corresponding states thermal conductivity (CSTC) correlation with both the influence of temperature and pressure is developed for ILs as follows

$$\lambda = \left(\frac{11.1}{T^x} + \frac{fT_{br}^y}{gM^z} \right) \left[1 - h \left(\frac{P}{P_c} \right)^{0.7} \right] \quad (20)$$


Figure 2. Experimental vs. calculated densities for 514 data of 490 ILs using the FC–CS method.

$$x = 1.091, y = 0.552, z = 0.5817, f = 0.6107, \\ g = 0.1369, h = 0.007$$

The constants x , y , z , f , g , and h were attained via the minimization of the following objective function

$$O.F. = \sum_{i=1}^{N_p} (\lambda_i^{\text{cal}} - \lambda_i^{\text{exp}})^2 \quad (21)$$

The AARD can be defined as follows

$$\text{AARD (\%)} = 100 \times \sum_{i=1}^{N_p} |\lambda_i^{\text{cal}} / \lambda_i^{\text{exp}} - 1.0| / N_p \quad (22)$$

Results and Discussion

Critical properties

The determined fragment increments with respect to the FC–CS method for calculating T_b , T_c , P_c , and V_c are summarized in Table 4. The predicted T_b , T_c , P_c , V_c , ω and ρ using the FC–CS method for 490 ILs are provided in the

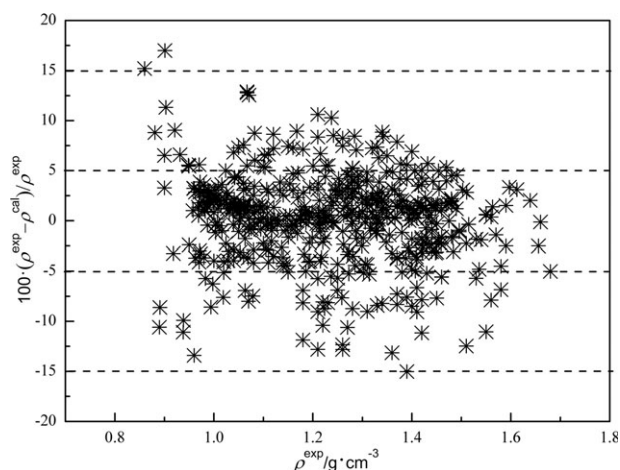

Figure 3. Relative deviations between the experimental and calculated densities as a function of experimental density.

Table 5. Comparison of the Calculated Density Deviations of ILs

Methods	NG ^d	ILs	Points	Min RD ^e (%)	Max RD(%)	Overall AARD(%)	Distributions of ARD ^f of the calculated densities of ILs		
							≤5.0%	5.0–10.0%	>10.0%
FC—CS ^a	46	490	514	−15	15.7	3.3	399	93	22
LGM ^b	44	294	294	−20.5	28.1	3.9	222	50	22
GC—PT ^c	47	747	918	−29.9	30.8	4.4	645	189	84

^aFC—CS: FC—CS Method proposed in this study.

^bLGM: Linear Generalized Method used in ref. 38.

^cGC—PT: GC—PT Method presented in ref. 17.

^dNG: Number of groups/fragments defined to calculate the critical properties.

^eRD: Relative deviation of density, $\Delta\rho(\%) = (\rho^{\text{cal}} - \rho^{\text{exp}})/\rho^{\text{exp}} \times 100$.

^fARD: Absolute relative deviation of density, $|\Delta\rho|(\%) = |(\rho^{\text{cal}} - \rho^{\text{exp}})/\rho^{\text{exp}}| \times 100$.

worksheet “Critical Properties” in the Supplementary Material. Figure 2 shows the comparison of the experimental and correlated densities using the FC—CS method. Figure 3 is the plot of the relative deviations between the calculated and experimental densities as a function of experimental density for all data points used in this study.

As can be seen in Figure 2, the calculated densities using the FC—CS method were in good agreement with the corresponding experimental densities with an overall AARD of 3.3%. As shown in Figure 3, majority of the relative deviations were within $\pm 10\%$ and distributed randomly around the baseline of 0%. These results indicate the validity of the calculated 46 fragment increments. The observed maximum relative deviation was 15.7% for [P₆₆₆₍₁₄₎][Tcm] (Trihexyltetradecylphosphonium tricyanomethanide) at 293.15 K and 101.3 kPa. Screening of the experimental density was not possible for [P₆₆₆₍₁₄₎][Tcm] because of the limited availability of data in literature. However, lower deviations can be found in other compounds with the same [P₆₆₆₍₁₄₎] cation or [Tcm] anion. For instance, the deviation was 1.0% for [C₄MIm][Tcm] (1-butyl-3-methyl-imidazolium tricyanomethanide) and 0.1% for [P₆₆₆₍₁₄₎][Ace] (tetradecyltriethylphosphonium acesulfamates), demonstrating that such a large deviation for IL [P₆₆₆₍₁₄₎][Tcm] is not caused by unsuitable fragment increments.

A comprehensive comparison of the accuracies of different methods, including total number of groups/fragments and ILs, overall AARD, maximum and minimum deviations, and distributions of ARD, are summarized in Table 5. As shown in Table 5, the FC—CS method presented in this study gives lower overall AARD and greater percentage of low deviations. All results suggest that the IL fragments defined in this study are successful in predicting critical points, at least

for the ILs studied in this section. The rationality of the critical properties derived using the FC—CS method should be further verified in the light of their potential to correlate with more property data, such as density over a wider condition and surface tension, as will be discussed in the subsequent sections of this study.

Density prediction using six CSP equations

With the fragment increments in Table 4, T_b , T_c , P_c , and V_c of 519 ILs were calculated using Eqs. 1–4. Considering that the fragment increments were derived solely from the density data of ILs at ambient temperature and atmospheric pressure, the densities at higher temperature and pressure should be estimated to verify the prediction performance of the developed FC—CS method. Based on the calculated data, the temperature dependence of the densities were predicted using six density equations, namely, Eq. 1 and Eqs. 9–13. The detailed results, including all calculated data and deviations, are provided in the worksheets named “Density Dependence of T” and “Density Dependence of P and T” in the Supplementary Material. As shown in Table 6, the six density equations obtained good predictive results for the 1,907 density data points of 519 ILs, especially the Riedel and YG equations with low AARDs of 2.1% and 2.3%, respectively. The AARD for the 3,272 density data points of 128 ILs was only 1.1% for the Riedel equation and 1.3% for the YG equation. The maximum relative deviation of 15.7% was observed for [P₆₆₆₍₁₄₎][Tcm] (Trihexyltetradecylphosphonium tricyanomethanide) by Riedel equation, whereas the LGM and the MH equation merely gave relative deviation of 1.8% and 0.9%, respectively, for the same data point. This implies some large deviations are caused by random errors of different predictive equations. Even so, Riedel and

Table 6. Comparison of the Calculated Density Deviations of ILs using Six Equations

Methods	Min RD(%)	Max RD(%)	Overall AARD(%)	Distributions of ARD of the calculated densities of ILs			
				≤1.0%	1.0–5.0%	5.0–10.0%	>10.0%
1907 data points in the temperature range of 273.15–473.15 K and pressure of 0.1 Mpa							
Riedel	−15.0	15.7	2.1	721	980	181	25
VSD	−21.9	33.6	4.4	262	1053	417	175
VSY	−24.0	17.9	3.7	305	1056	507	39
LGM	−29.5	17.9	3.8	301	1066	477	63
YG	−16.4	45.3	2.3	737	940	191	39
MH	−36.5	7.1	5.8	116	789	797	205
3272 data points in the temperature range of 278.15–428.15 K and pressure range of 0.1–100 MPa							
Riedel	−4.9	5.0	1.1	1665	1607	0	0
VSD	−6.6	10.2	3.6	293	2131	845	3
VSY	−9.4	3.7	2.9	541	2194	537	0
LGM	−5.3	12.5	3.1	474	2230	544	24
YG	−5.0	4.9	1.3	1581	1690	1	0
MH	−12.0	2.4	4.8	220	1725	1173	154

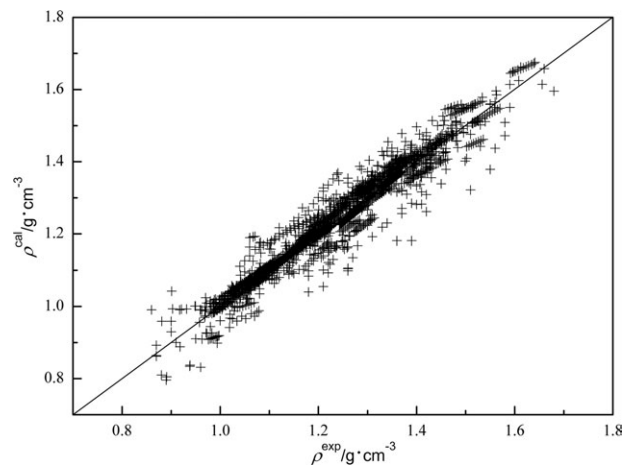


Figure 4. Experimental vs. calculated densities using the Riedel equation for 1,907 data of 519 ILs.

YG equation are recommended to predict density based on critical properties derived from the FC—CS model, because they usually obtain more accurate predictive results in most cases. Some deflected experimental data may also cause large deviations. For example, three different relative deviations can be found for [C₄Py][BTI] (1-butylpyridinium bis(trifluoromethylsulfonyl)imide). Among them, the largest is -6.5% which is caused by the inaccuracy of experimental data when compared with the other two of -3.2% and -3.3% . However, relative deviations of ILs composed of alanine based cation and nitrate anion are larger than 12% using all the six density equations. So the FC—CS method is not recommended to be used for this kind of IL. On the whole, large deviations can mainly be attributed to two factors, namely (1) random error of a density prediction equation, and (2) the inaccuracy of the experimental data.

As shown in Figure 4, the calculated densities for 519 ILs were randomly distributed along the diagonal $\rho^{\text{cal}} = \rho^{\text{exp}}$. Figure 5 clearly shows that majority of the deviations were within $\pm 5\%$, and the deviations were distributed randomly around the baseline of 0% . Similar results can be found for 128 ILs over a wide pressure range, as shown in Figures 6 and 7. The results suggest that the FC—CS method is valid and the derived critical properties can be successfully applied to predict density of ILs using different corresponding states correlations.

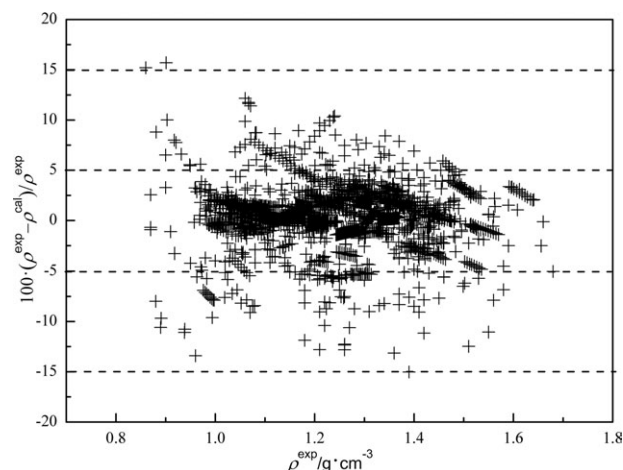


Figure 5. Relative deviations between the experimental and calculated densities for the same data set as in Figure 4.

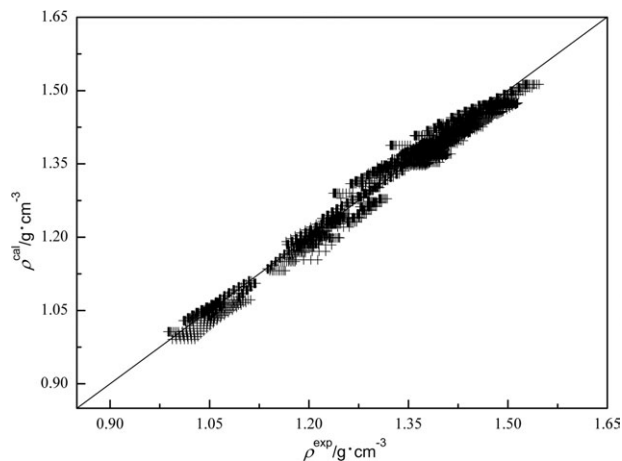


Figure 6. Experimental vs. calculated densities using the Riedel equation for 3,272 data of 128 ILs.

Surface tension prediction using two CSP equations

The surface tensions of 112 ILs at varying temperatures were predicted using the Brock-Bird equation (see Eq. 14), and Pitzer equation (see Eq. 15), to further validate the calculated critical properties using the FC—CS method. Figures 8a and 8b show the comparisons of the experimental and calculated surface tensions using the Brock-Bird and Pitzer equations, respectively. The 838 experimental surface tension data of 112 pure ILs were found to be in accordance with the predicted values using the Brock-Bird and Pitzer equations with overall AARDs of 3.7% and 3.6% , respectively. The maximum deviations of the Brock-Bird and Pitzer equations were -12.3% and -25.9% for [N₈₈₈₁][BTI] (trioctyl(methyl)ammonium bis(trifluoromethylsulfonyl)imide) and [(NH₂)C₄C₁im][BF₄] (1-(4-Aminobutyl)-3-methylimidazolium dicyanamide), respectively. The maximum deviations are probably caused by the random error of different predictive equations, because the other equation gives low RD of -3.7% and -8.1% , respectively. The results further indicate that the FC—CS method is reliable and the obtained critical properties can be used satisfactorily in predicting surface tension using different corresponding states correlations.

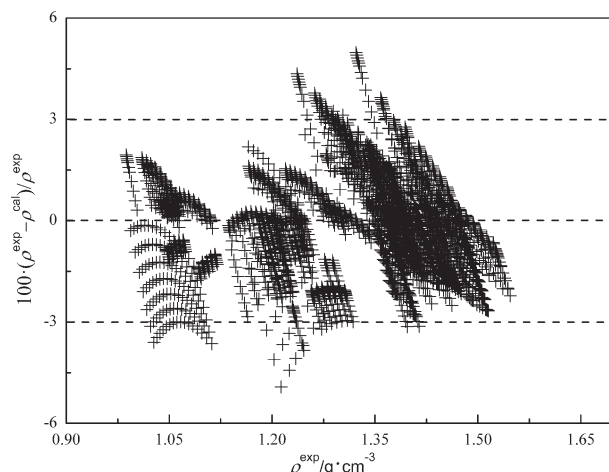


Figure 7. Relative deviations between the experimental and calculated densities for the same data set as in Figure 6.

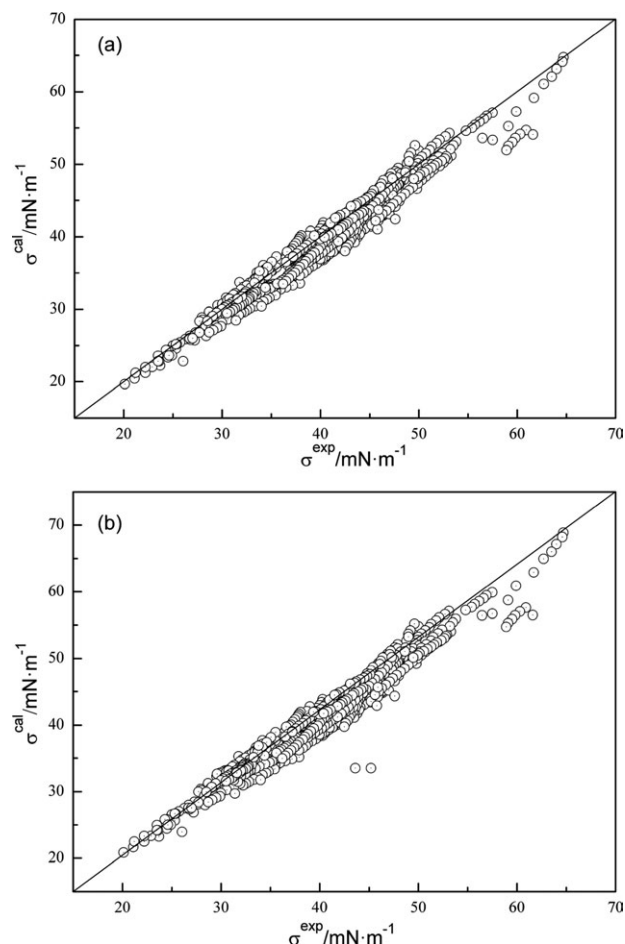


Figure 8. Experimental vs. calculated surface tensions of 112 ILs within the temperature range of 273.15 K to 492.5 K using the (a) Brock-Bird equation, and (b) Pitzer equation.

The surface tension of 24 ILs were calculated using the Brock-Bird and Pitzer equations based on the critical properties obtained by Valderrama³⁸ and the FC—CS method, respectively to compare the performances of the two methods. Figure 9a and 9b show the relative deviation RD (%) of surface tension based on different critical properties sources. Detailed results are shown in the worksheet named “Comparison with Valderrama” in the Supplementary Material. The maximum relative deviations of FC—CS method and Valderrama in calculating surface tension were -8.3% and 88.5% ,

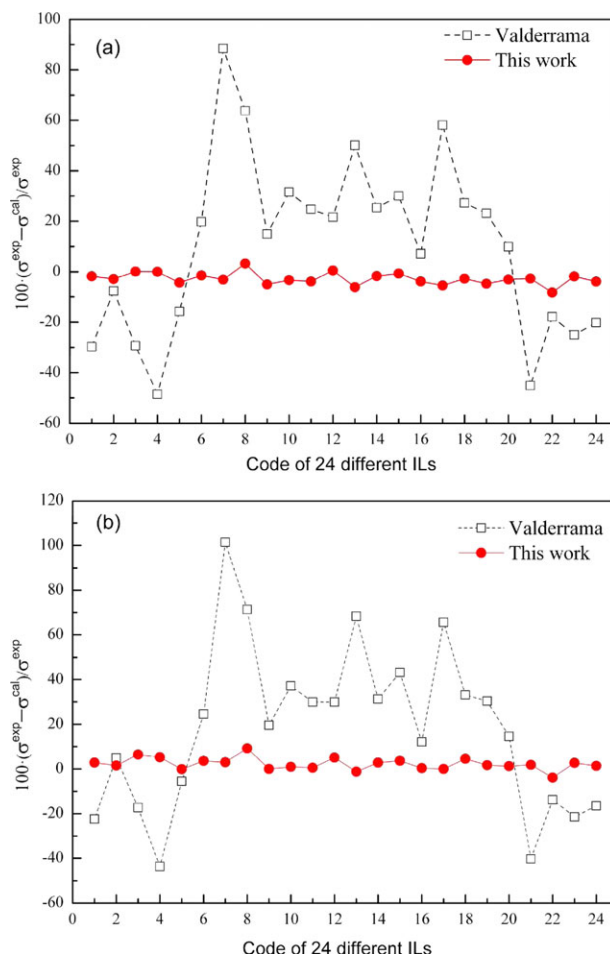


Figure 9. Critical properties from Valderrama and the current study led to different deviations between the experimental and calculated surface tension data using the (a) Brock-Bird equation, and (b) Pitzer equation.

[Color figure can be viewed in the online issue, which is available at wileyonlinelibrary.com.]

respectively. The results indicate that the FC—CS method was improved for predicting critical properties of ILs.

Applicability for mixtures of ILs

Experimental density data of 13 kinds of binary ILs were obtained from literature,^{57–59} and their critical properties and

Table 7. The Calculated Density Deviations of Binary ILs Mixtures by Riedel Equation

Binary mixtures	x_1 (mole fraction)	T/K	Points	Min RD (%)	Max RD (%)	AARD (%)
[C ₆ MIm][BF ₄](1) + [C ₂ MIm][BF ₄](2)	0.0978–0.9455	298	13	−0.2	0.4	0.3
[C ₄ MIm][BF ₄](1) + [C ₄ MIm][MeSO ₄](2)	0.1209–0.9683	308	14	−0.1	0.2	0.1
[C ₄ MIm][BF ₄](1) + [C ₆ MIm][BF ₄](2)	0.1083–0.946	301	10	−3.2	4.6	2.1
[C ₄ MIm][PF ₆](1) + [C ₄ MIm][BF ₄](2)	0.0568–0.945	303	12	0.2	0.3	0.3
[omim][BF ₄](1) + [omim][Cl](2)	0.2–0.8	303–333	20	−0.3	0.3	0.2
[hmim][BF ₄](1) + [hmim][Cl](2)	0.2–0.8	303–333	16	−0.2	0.3	0.2
[hmim][PF ₆](1) + [hmim][Cl](2)	0.2–0.8	303–333	16	−0.1	0.6	0.3
[C ₁ MPyr][BTI](1) + [C ₄ MPyr][BTI](2)	0.1–0.4	273–373	4	−0.8	1.3	0.8
[C ₁ MPyr][BTI](1) + [C ₅ MPyr][BTI](2)	0.1–0.3	283–373	3	0	2.2	0.8
[C ₂ MPyr][BTI](1) + [C ₃ MPyr][BTI](2)	0.1–0.5	283–373	5	−0.9	1.1	0.7
[C ₂ MPyr][BTI](1) + [C ₄ MPyr][BTI](2)	0.1–0.5	273–373	5	−1.1	1.2	0.8
[C ₂ MPyr][BTI](1) + [C ₅ MPyr][BTI](2)	0.1–0.5	273–373	5	−0.3	1.6	0.8
[C ₃ MPyr][BTI](1) + [C ₅ MPyr][BTI](2)	0.1–0.9	273–373	5	−1.7	1.6	0.7
Total	0.0568–0.9683	273–373	128	−0.7	1.2	0.6

densities were predicted. The predicted values display well agreement with experimental data, as shown in Table 7. The results suggest the FC—CS method is also applicable for mixtures of ILs. More details of the calculation can be found in “Mixtures of ILs” of Supplementary Material.

Heat capacity

Based on the critical properties calculated above, 599 liquid heat capacity data of 26 ILs that cover a wide temperature range (10 K to 573.10 K) were estimated using the CSHC correlation (see Eq. 17) proposed in this study. The calculated liquid heat capacities agree well with the corresponding experimental data with an overall AARD of 3.8%, as shown in Figure 10. Although the obtained AARD was higher than the AARD of 2.9% reported by Ge et al.³⁰ the temperature range of the data points was wider, i.e., the CSHC equation can be applied under broader conditions. All relative deviations of the 599 calculated data points were within $\pm 10.0\%$, of which 64% were within ± 5.0 and 36% were between $\pm(5.0$ and $10.0)$ %. Moreover, the maximum deviations were 9.9% observed for $[C_4MIm][Br]$ (1-Butyl-3-methylimidazolium Bromide) at an extremely low temperature (110 K). The detailed results are described in the worksheet “Heat capacity” in the Supplementary Material.

Thermal conductivity

Almost all available thermal conductivity data in literature were collected, including 22 ILs within the temperature range of 273.15 K to 390 K and 0.1 MPa to 20 MPa pressure. The thermal conductivities of the 22 ILs were between 0.117 and 0.205, which were near $0.10 \text{ W}\cdot\text{m}^{-1}\cdot\text{K}^{-1}$ to $0.17 \text{ W}\cdot\text{m}^{-1}\cdot\text{K}^{-1}$ range of most organic liquids below the normal boiling point.²⁰ The CSTC correlation (see Eq. 20) was proposed to predict the dependence of thermal conductivity on temperature and pressure. Figure 11 shows the relative deviations between the calculated and experimental data as a function of experimental value for all data points used in the current study. As shown in Figure 11, all deviations were within $\pm 10\%$, and were distributed randomly around the baseline of 0%, among which 74% were within ± 5.0 , and 26% were between $\pm(5.0$ and $10.0)$ %. The detailed results are described in the worksheet “Thermal conductivity” in the Supplementary Material.

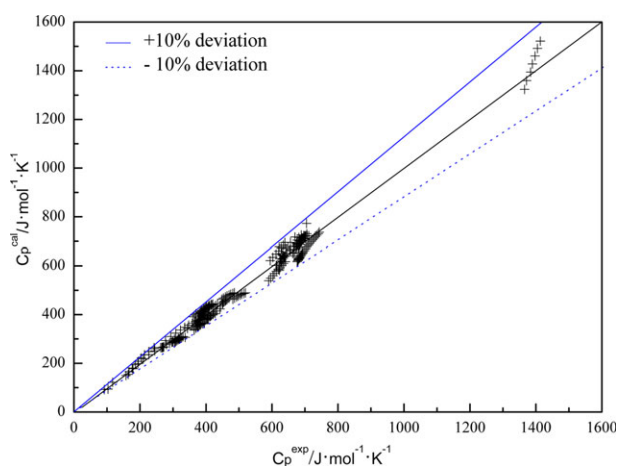


Figure 10. Comparison between the predicted and experimental heat capacities of 26 ILs within the temperature ranges of 10 K to 573.1 K.

[Color figure can be viewed in the online issue, which is available at wileyonlinelibrary.com.]

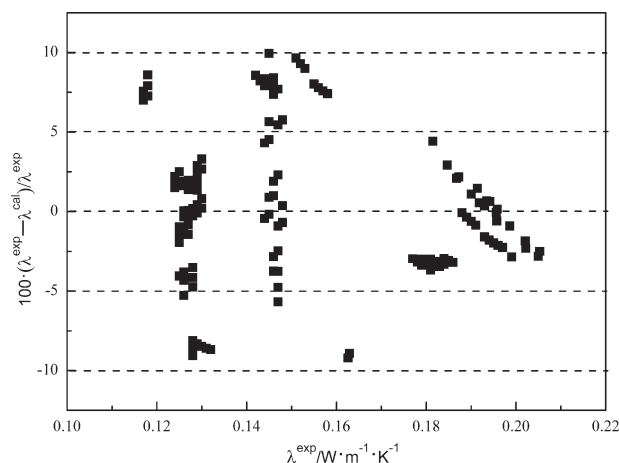


Figure 11. Relative deviations between the experimental and calculated thermal conductivities of 26 ILs.

Conclusions

This study developed a FC—CS method on the basis of 46 fragments for the prediction of the normal boiling temperatures, critical properties, and acentric factors of ILs. The fragment increments were determined using the experimental density data of 490 pure ILs under ambient temperature and atmospheric pressure. It shows the FC—CS method provides more reliable prediction results than the original GCM with neutral groups, given that both the temperature and pressure dependence of the density and surface tension of ILs can be correlated well using different equations. Those results imply that the definition of fragments and the estimated critical properties of pure ILs are reasonable. Furthermore, the method is able to be applied for mixtures of ILs.

The heat capacity and thermal conductivity of ILs can be successfully predicted using the CSHC and CSTC correlations proposed in this study by virtue of critical parameters calculated by the FC—CS method, at least for the ILs investigated. Compared with any other reported methods, the correlations exhibited general feasibility since they were obtained based on the CSP.

The methods and correlations proposed in this study take advantage of both the convenience of GCM and the generalized applicability of CSP, and will be useful for the acquisition of physicochemical properties for ILs at least investigated here. The FC—CS method will allow new IL fragment to be defined to predict critical properties of other ILs when their experimental density data are available. With the derived critical properties, more CSP correlations and equations of state can be developed to play a fundamental role in exploiting new process using ILs.

Acknowledgments

This work was financially supported by Key Program of National Natural Science Foundation of China (No. 21036007), by the National High Technology Research and Development Program of China (No. 2011AA050606), and by the Petrochemical Joint Funds of NSFC—CNPC (No. U1162105).

Notation

Symbols

- C_p = liquid heat capacity, $\text{J}\cdot\text{mol}^{-1}\cdot\text{K}^{-1}$
- M = molar mass, $\text{g}\cdot\text{mol}^{-1}$
- N_p = total number of data points
- P_b = normal boiling pressure, 1.01325 bar

P_c = critical pressure, bar
 T_b = normal boiling temperature, K
 T_{br} = reduced temperature at the normal boiling point
 T_c = critical temperature, K
 T_r = reduced temperature
 V_c = critical volume, $\text{cm}^3\text{mol}^{-1}$

Abbreviations

AARD = average absolute relative deviation
CSP = corresponding states principle
CSHC = corresponding states heat capacity correlation proposed
CSTC = corresponding states thermal conductivity correlation proposed
GCM = group contribution method
FC—CS = fragment contribution—corresponding states
IL = ionic liquid
LGM = near generalized model by Valderrama et al.
MH = Mchaweh et al. equation
QSPR = quantitative structure–property relationship
RD = relative deviation
VSD = Valderrama and Abu-Sharkh SD equation
VSY = Valderrama and Abu-Sharkh SY equation
YG = Yamada and Gunn equation

Greek letters

ρ = density, $\text{g}\cdot\text{cm}^{-3}$
 σ = surface tension, $\text{mN}\cdot\text{m}^{-1}$
 λ = liquid thermal conductivity, $\text{W}\cdot\text{m}^{-1}\cdot\text{K}^{-1}$
 ω = acentric factor

Subscripts

cal = calculated property
exp = experimental property

Literature Cited

- Rogers RD, Seddon KR. Ionic liquids - Solvents of the future? *Science*. 2003;302:792–793.
- Welton T. Room-temperature ionic liquids. Solvents for synthesis and catalysis. *Chem Rev*. 1999;99:2071–2083.
- Yang Z, Pan WB. Ionic liquids: Green solvents for nonaqueous biocatalysis. *Enzyme Microb Technol*. 2005;37:19–28.
- Endres F. Ionic liquids: Solvents for the electrodeposition of metals and semiconductors. *Chemphyschem*. 2002;3:144–154.
- Pandey S. Analytical applications of room-temperature ionic liquids: A review of recent efforts. *Anal Chim Acta*. 2006;556:38–45.
- Allen D, Baston G, Bradley AE, Gorman T, Haile A, Hamblett I, Hatter JE, Healey MJF, Hodgson B, Lewin R, Lovell KV, Newton B, Pitner WR, Rooney DW, Sanders D, Seddon KR, Sims HE, Thied RC. An investigation of the radiochemical stability of ionic liquids. *Green Chem*. 2002;4:152–158.
- Han X, Armstrong DW. Ionic liquids in separations. *Acc Chem Res*. 2007;40:1079–1086.
- Trohalaki S, Pachter R, Drake GW, Hawkins T. Quantitative structure–property relationships for melting points and densities of ionic liquids. *Energy Fuel*. 2005;19:279–284.
- Sun N, He X, Dong K, Zhang X, Lu X, He H, Zhang S. Prediction of the melting points for two kinds of room temperature ionic liquids. *Fluid Phase Equilib*. 2006;246:137–142.
- Palomar J, Ferro VR, Torrecilla JS, Rodriguez F. Density and molar volume predictions using COSMO-RS for ionic liquids. An approach to solvent design. *Ind Eng Chem Res*. 2007;46:6041–6048.
- Torrecilla JS, Palomar J, Garcia J, Rodriguez F. Effect of cationic and anionic chain lengths on volumetric, transport, and surface properties of 1-Alkyl-3-methylimidazolium alkylsulfate ionic liquids at (298.15 and 313.15) K. *J Chem Eng Data*. 2009;54:1297–1301.
- Diedenhofen M, Klamt A, Marsh K, Schaefer A. Prediction of the vapor pressure and vaporization enthalpy of 1-n-alkyl-3-methylimidazolium-bis-(trifluoromethanesulfonyl) amide ionic liquids. *Phys Chem Chem Phys*. 2007;9:4653–4656.
- Jacquemin J, Husson P, Padua AAH, Majer V. Density and viscosity of several pure and water-saturated ionic liquids. *Green Chem*. 2006;8:172–180.
- Guerrero H, Martín S, Pérez-Gregorio V, Lafuente C, Bandrés I. Volumetric characterization of pyridinium-based ionic liquids. *Fluid Phase Equilib*. 2012;317:102–109.
- Koller T, Rausch MH, Schulz PS, Berger M, Wasserscheid P, Economou IG, Leipertz A, Fröba AP. Viscosity, interfacial tension, self-diffusion coefficient, density, and refractive index of the ionic liquid 1-ethyl-3-methylimidazolium tetracyanoborate as a function of temperature at atmospheric pressure. *J Chem Eng Data*. 2012;57:828–835.
- Fröba AP, Rausch MH, Krzeminski K, Assenbaum D, Wasserscheid P, Leipertz A. Thermal conductivity of ionic liquids: measurement and prediction. *Int J Thermophys*. 2010;31:2059–2077.
- Shen C, Li CX, Li XM, Lu YZ, Muhammad Y. Estimation of densities of ionic liquids using Patel-Teja equation of state and critical properties determined from group contribution method. *Chem Eng Sci*. 2011;66:2690–2698.
- Paduszynski K, Domanska U. A new group contribution method for prediction of density of pure ionic liquids over a wide range of temperature and pressure. *Ind Eng Chem Res*. 2012;51:591–604.
- Gardas RL, Coutinho JAP. Group contribution methods for the prediction of thermophysical and transport properties of ionic liquids. *AIChE J*. 2009;55:1274–1290.
- Poling BE, Prausnitz JM, John Paul OC. *The properties of gases and liquids*. New York: McGraw-Hill; 2001.
- Eslami H. Prediction of the density for natural gas and liquefied natural gas mixtures. *AIChE J*. 2001;47:2585–2592.
- Guggenheim EA. The principle of corresponding states. *J Chem Phys*. 1945;13:253–261.
- Escobedo J, Mansoori GA. Surface-tension prediction for liquid mixtures. *AIChE J*. 1998;44:2324–2332.
- Nagasaka Y, Nagashima A. Corresponding states correlation for the thermal conductivity of molten alkali halides. *Int J Thermophys*. 1993;14:923–936.
- Kim W, Lee S. A corresponding state theory for the viscosity of liquids. *Bull Korean Chem Soc*. 2008;29:33–37.
- Janz GJ, Yamamura T, Hansen MD. Corresponding-states data correlations and molten salts viscosities. *Int J Thermophys*. 1989;10:159–171.
- Hwang MJ, Whiting WB. A corresponding-states treatment for the viscosity of polar fluids. *Ind Eng Chem Res*. 1987;26:1758–1766.
- Valderrama JO, Zarricueta K. A simple and generalized model for predicting the density of ionic liquids. *Fluid Phase Equilib*. 2009;275:145–151.
- Mousazadeh M, Faramarzi E. Corresponding states theory for the prediction of surface tension of ionic liquids. *Ionics*. 2011;17:217–222.
- Ge R, Hardacre C, Jacquemin J, Nancarrow P, Rooney DW. Heat capacities of ionic liquids as a function of temperature at 0.1 MPa. measurement and prediction. *J Chem Eng Data*. 2008;53:2148–2153.
- Shereshfetsky J. Surface Tension of Saturated Vapors and the Equation of eötvös. *J Phys Chem*. 1931;35:1712–1720.
- Rebelo LPN, Lopes JNC, Esperanca JMSS, Filipe E. On the critical temperature, normal boiling point, and vapor pressure of ionic liquids. *J Phys Chem B*. 2005;109:6040–6043.
- Weiss VC. Guggenheim's rule and the enthalpy of vaporization of simple and polar fluids, molten salts, and room temperature ionic liquids. *J Phys Chem B*. 2010;114:9183–9194.
- Kilaru P, Baker GA, Scovazzo P. Density and surface tension measurements of imidazolium-, quaternary phosphonium-, and ammonium-based room-temperature ionic liquids: data and correlations. *J Chem Eng Data*. 2007;52:2306–2314.
- Ghatee MH, Moosavi F, Zolghadr AR, Jahromi R. Critical-point temperature of ionic liquids from surface tension at liquid-vapor equilibrium and the correlation with the interaction energy. *Ind Eng Chem Res*. 2010;49:12696–12701.
- Weiss VC, Heggen B, Müller-Plathe F. Critical parameters and surface tension of the room temperature ionic liquid [bmim][pf6]: a corresponding-states analysis of experimental and new simulation data. *J Phys Chem C*. 2010;114:3599–3608.
- Valderrama JO, Robles PA. Critical properties, normal boiling temperatures, and acentric factors of 50 ionic liquids. *Ind Eng Chem Res*. 2007;46:1338–1344.
- Valderrama JO, Rojas RE. Critical properties of ionic liquids. Revisited. *Ind Eng Chem Res*. 2009;48:6890–6900.
- Jones RG, Licence P, Lovelock KRI, Villar-Garcia IJ. Comment on “Critical properties, normal boiling temperatures, and acentric factors of 50 ionic liquids”. *Ind Eng Chem Res*. 2007;46:6061–6062.
- Ionic Liquids Database (ILThermo). NIST Standard Reference Database #147. National Institute of Standards and Technology, Standard Reference Data Program, Gaithersburg, MD, 2010. <http://ILThermo.boulder.nist.gov/ILThermo/>.

41. Zhang S, Lu X, Zhou Q, Li X, Zhang X. *Ionic Liquids: Physicochemical Properties*. New York: Elsevier Science; 2009.
42. Zhang S, Lu X, Zhou Q, Li X, Zhang X. *Ionic Liquid Database software*. Beijing: Group of Ionic Liquids Clean Process and Energy-saving; 2010.
43. Tariq M, Freire MG, Saramago B, Coutinho JAP, Lopes JNC, Rebelo LPN. Surface tension of ionic liquids and ionic liquid solutions. *Chem Soc Rev*. 2012;41:829–868.
44. Zhang Q, Li Z, Zhang J, Zhang S, Zhu L, Yang J, Zhang X, Deng Y. Physicochemical properties of nitrile-functionalized ionic liquids. *J Phys Chem B*. 2007;111:2864–2872.
45. Ries LAS, do Amaral FA, Matos K, Martini EMA, de Souza MO, de Souza RF. Evidence of change in the molecular organization of 1-n-butyl-3-methylimidazolium tetrafluoroborate ionic liquid solutions with the addition of water. *Polyhedron*. 2008;27:3287–3293.
46. Riedel L. Liquid density in the saturated state. extension of the theorem of corresponding states II. *Chem Ing Tech*. 1954;26:259–264.
47. Joback KG, Reid RC. Estimation of pure-component properties from group-contributions. *Chem Eng Commun*. 1987;57:233–243.
48. Alvarez V, Valderrama J. A modified Lydersen-Joback-Reid method to estimate the critical properties of biomolecules. *Alimentaria*. 2004;254:55–66.
49. Ma P, Xu M, Xu W, Zhang J. New group contribution correlations for estimation of critical properties. *Chinese J Chem Eng*. 2000;8:74–79.
50. Valderrama JO, Abu-Sharkh BF. Generalized rackett-type correlations to predict the density of saturated liquids and petroleum fractions. *Fluid Phase Equilib*. 1989;51:87–100.
51. Yamada T, Gunn RD. Saturated liquid molar volumes. Rackett equation. *J Chem Eng Data*. 1973;18:234–236.
52. McHaweh A, Alsaygh A, Nasrifar K, Moshfeghian M. A simplified method for calculating saturated liquid densities. *Fluid Phase Equilib*. 2004;224:157–167.
53. Queimada AJ, Marrucho IM, Coutinho JAP. Surface tension of pure heavy n-alkanes: a corresponding states approach. *Fluid Phase Equilib*. 2001;183:229–238.
54. Dee GT, Sauer BB. The surface tension of polymer liquids. *Adv Phys*. 1998;47:161–205.
55. Rice P, Teja AS. A generalized corresponding-states method for the prediction of surface tension of pure liquids and liquid mixtures. *J Colloid Interf Sci*. 1982;86:158–163.
56. Brock JR, Bird RB. Surface tension and the principle of corresponding states. *AIChE J*. 1955;1:174–177.
57. Ning H, Hou M, Mei Q, Liu Y, Yang D, Han B. The physicochemical properties of some imidazolium-based ionic liquids and their binary mixtures. *Sci China Chem*. 2012;1–10.
58. Navia P, Troncoso J, Romani L. Excess magnitudes for ionic liquid binary mixtures with a common ion. *J Chem Eng Data*. 2007;52:1369–1374.
59. Fox ET, Weaver JEF, Henderson WA. Tuning binary ionic liquid mixtures: linking alkyl chain length to phase behavior and ionic conductivity. *J Phys Chem C*. 2012;116:5270–5274.

Manuscript received May 31, 2012, and revision received Aug. 7, 2012.